Accepted Manuscript

Probabilistic assessment of performance under uncertain information using a generalised maximum entropy principle

Alice Cicirello, Robin S. Langley

PII: S0266-8920(17)30062-0
DOI: http://dx.doi.org/10.1016/j.probengmech.2017.07.006
Reference: PREM 2936

To appear in: *Probabilistic Engineering Mechanics*

Received date : 23 March 2017
Revised date : 8 June 2017
Accepted date : 25 July 2017

Please cite this article as: A. Cicirello, R.S. Langley, Probabilistic assessment of performance under uncertain information using a generalised maximum entropy principle, *Probabilistic Engineering Mechanics* (2017), http://dx.doi.org/10.1016/j.probengmech.2017.07.006

Probabilistic assessment of performance under uncertain information using a generalised maximum entropy principle

Alice Cicirello[1*], Robin S. Langley[2]

[1] Department of Engineering Science
University of Oxford
Parks Road, Oxford OX1 3PJ
alice.cicirello@eng.ox.ac.uk

[2] Department of Engineering
University of Cambridge
Trumpington Street, Cambridge CB2 1PZ
rsl21@eng.cam.ac.uk

Abstract

When information about a distribution consists of statistical moments only, a self-consistent approach to deriving a subjective probability density function (pdf) is Maximum Entropy. Nonetheless, the available information may have uncertainty, and statistical moments maybe known only to lie in a certain domain. If Maximum Entropy is used to find the distribution with the largest entropy whose statistical moments lie within the domain, the information at only a single point in the domain would be used and other information would be discarded. In this paper, the bounded information on statistical moments is used to construct a family of Maximum Entropy distributions, leading to an uncertain probability function. This uncertainty description enables the investigation of how the uncertainty in the probabilistic assignment affects the predicted performance of an engineering system with respect to safety, quality and design constraints. It is shown that the pdf which maximizes (or equivalently minimizes) an engineering metric is potentially different from the pdf which maximizes the entropy. The feasibility of the proposed uncertainty model is shown through its application to: (i) fatigue failure analysis of a structural joint; (ii) evaluation of the probability that a response variable of an engineering system exceeds a critical level, and (iii) random vibration.

Keywords: Maximum Entropy, uncertain probability density function, inequality constraints on statistical moments, bounds on failure probability, bounds on performance metric.

*Corresponding author: Department of Engineering Science, University of Oxford, Parks Road, Oxford OX1 3PJ, United Kingdom. *E-mail address:* alice.cicirello@eng.ox.ac.uk (Alice Cicirello).

1 Introduction

In engineering, several parameters of a computational model (such as geometry, material properties, loadings, boundary conditions, and structural joints) used to investigate the behaviour of a system may not be known precisely, and yet an engineering assessment of a design must nonetheless be performed. These uncertainties can be modelled in a parametric [1,2] or non-parametric way [2-5], or a combination of both [6-9]. While parametric approaches consider specific physical properties of the system to be uncertain, the non-parametric approaches account for the uncertainty effects at a higher level. Parametric uncertainty models can be probabilistic [1] or non-probabilistic (such as intervals [10], convex [11], and fuzzy [12]) and they are used in conjunction with a computational model to compute the effects of the uncertainties on the response.

The most widely used parametric uncertainty description is the probabilistic one based on a specified probability density function (pdf). This description requires a large amount of data if the pdf is constructed using a frequentist view, or it may be interpreted as a statement of belief based on expert opinion, as in the subjective approach to probability theory. The more common frequentist approach is concerned with the outcome of experiments performed (hypothetically or in reality) on large ensembles of systems; these ensembles may either be real (for example cars from a production line), or virtual but realizable in principle (such as an ensemble of manufactured satellites, when only one satellite may actually be built). In contrast, with the subjective approach, no ensemble is necessarily involved. The pdf is interpreted as a statement of belief, rather than a frequentist statement, meaning that the analyst can specify a pdf in the absence of large quantities of data. The frequentist and subjective views can be roughly aligned with the notion of aleatory and epistemic uncertainty: aleatory uncertainty is an irreducible uncertainty due to an inherent variability of the system parameters, while epistemic uncertainty is reducible, being associated to a lack of knowledge of the actual values of the parameters which are fixed.

In the frequentist case there is often insufficient data to empirically determine the pdf, due to cost or time constraints, and it may not be possible to take measurements if the structure does not yet exist. Similarly, in the subjective case, the analyst may have uncertainties in belief, meaning that the specified pdf is itself subject to doubt. Alternative uncertainty models have been developed by introducing uncertainty in the assignment of the parameters of a probability density function (pdf), and/or the pdf itself. These models are broadly referred to as "imprecise probability approaches". The idea of specifying upper and lower bounds on an imprecisely known probability of an event was introduced about 100 years ago by Boole [13] and Keynes [14]. Later, Walley [15] and Weichselberger [16] developed generalized probability theories. The imprecise probability approaches which are most widely used can be broadly classified into five groups: (i) Probability boxes [17,18]; (ii) Possibility theory [19,20], (iii) Evidence theory [21-25], (iv) Imprecise pdf descriptions based on the specification of interval constraints on the expectation of functions of the uncertain variable, such as the approach proposed by Utkin and co-workers [26,27]; (v) Probability and cumulative density functions (pdf and cdf) with non-probabilistic parameters (i.e. interval, convex, fuzzy descriptions), such as: (a) Parameterized P-Box [28]; (b) Fuzzy probability theory (also known as Fuzzy randomness) [29-31]; (c) Fuzzy random variable [32, 32]; (d) First Order Reliability Method (FORM) [1] approaches which employ pdfs with one [34] or two [35] bounded parameters (mean, variance or another distribution parameter); (e) Reliability models based on imprecise Bayesian inference models [36]; (f) Interval importance sampling methods combined with specified pdf with bounded parameters [37].

Another way of dealing with limited information about a distribution is Maximum Entropy [38]. Maximum Entropy is a well-established approach to deriving a subjective probability density function (pdf) using statistical moments information only. However, there might be little confidence on statistical moments estimated from a small data set. Moreover, if no data is available and the pdf is interpreted as a statement of belief, the analyst may have uncertainties in belief and might prefer not to specify exact statistical moments. Therefore, statistical moments might be known only to lie in a certain domain, rather than being precisely known. In this case Maximum Entropy would select a unique distribution which maximises the entropy and whose statistical properties are within the statistical moment domain [38,39]. However, in this process some of the initial information is lost, since only one point of the statistical moment domain would be considered and other points, to which correspond different pdfs, are discarded. However, the pdf which maximizes (or equivalently minimizes) an engineering metric is potentially different from the pdf which maximizes the entropy.

A new approach to uncertainty modelling which is based on a generalization of maximum entropy theory is presented in this paper, and applied to a number of engineering examples. With this approach, when the statistical moments are known only to lie in a certain domain, instead of selecting the pdf which maximize the entropy, a family of Maximum Entropy distributions is constructed. This is achieved by representing the pdf of the vaguely known variable as the exponential of a linear combination of functions of the uncertain variable and bounded parameters. This form is equivalent to the Maximum entropy distribution, where the Lagrange multipliers (which are constant values) are substituted by bounded parameters, leading to a set of pdfs. These bounded parameters are referred to as basic variables, defined as having any form of distribution lying between certain bounds, encompassing at the extreme a delta function at any point between the bounds. A mapping procedure is devised to convert bounded information on the statistical moments into bounds on the basic variables. With this approach a bounded response description is then obtained by maximising (minimising) a response metric over the set of pdfs to: (i) establish the effects of the imprecisely known pdf on the response; and (ii) identify of the worst case scenario (e.g. the highest failure probability expected).

The present approach has similarities to that proposed by Utkin [26,27], in that the information considered is a set of constraints on the statistical moments. However, in [26,27] the set of moments yield to many possible distributions with no consideration of Entropy, and a set of complex optimization problems is performed to yield bounds on the expectation of the response or on the reliability of the system, which restrict its application to simple problems. Instead, within the proposed approach, the specified set of constraints are used to: (i) identify the form of the Maximum Entropy distribution, and to (ii) yield bounds on the basic variables of the pdf to construct a set of maximum entropy pdfs.

As described above, the main aim of the present paper is to present a generalisation of the Maximum Entropy principle given uncertain statistical information, leading to a family of probability distributions that can be used to make engineering judgements. The theory behind this approach is presented in Section 2, with a numerical example of the treatment of bounded information in Section 2.2.4. Attention is then turned to three engineering applications, namely the fatigue failure of a structural joint (section 3.1), the overstress failure of a structural joint (section 3.2), and the random vibration of an oscillator (section 3.3). Aspects of theory relating specifically to the example applications are contained in the relevant subsections, to emphasise the fact that the theory presented in Section 2 is general, and not directed at any specific example.

2. Generalized Maximum Entropy distribution under uncertain statistical information

In subsection 2.1 the procedure for deriving a probability density function with the Maximum Entropy principle is first reviewed. The approach is then generalised to account for uncertainty in the statistical moments in subsection 2.2.

2.1 Review of Maximum Entropy

The principle of Maximum Entropy [38] allows the construction of a subjective pdf $p(x)$ of an uncertain variable x [38] which incorporates the current state of knowledge by maximizing the relative entropy subject to constraints representing the available information.
The relative entropy, that is the amount of uncertainty in the probability distribution $p(x)$, is given by [38]:

$$H = -\int_{-\infty}^{+\infty} p(x) \log\left(\frac{p(x)}{t(x)}\right) \mathrm{d}\, x \tag{1}$$

where $t(x)$ is a reference pdf (which is also known as the prior distribution) introduced to allow the entropy to be frame invariant [38, 40]

The available information regarding the statistics of the variable *x* is expressed in terms of *n* equality constraints on the statistical expectations in the form:

$$\mathrm{E}\left[f_j(x) \right] = \int_{-\infty}^{+\infty} f_j(x)\, p(x)\, \mathrm{d}\, x \qquad j = 2,3,\dots,n \tag{2}$$

where $f_j(x)$ are specified functions of *x*, and $\mathrm{E}\left[f_j(x) \right]$ is the statistical expectation of $f_j(x)$. If $f_j(x) = x$ then the constraints are specified on the mean value, alternatively if $f_j(x) = x^2$ they are specified on the second moment. The function $f_j(x)$ can be also defined as an interval of possible values that the uncertain variable may take, i.e. $f_j(x) = [b, c]$; in this case the constraints corresponds to the probability of finding *x* within those bounds.

This constrained maximization problem (maximizing Eq. (1) subject to Eq. (2)) can be solved by using the method of Lagrange multipliers [38], which is based on transforming the original constrained optimization problem into an unconstrained dual optimization problem in the form:

$$-\int_{-\infty}^{+\infty} p(x) \log\left(\frac{p(x)}{t(x)} \right) \mathrm{d}\, x + \sum_{j=1}^{n} \lambda_j \left\{ \int_{-\infty}^{+\infty} f(x)\, p(x)\, \mathrm{d}\, x - \mathrm{E}\left[f_j(x) \right] \right\} \tag{3}$$

where λ_j are the *n* Lagrange multipliers. The maximization of the functional in Eq. (3) is then obtained using the calculus of variations, which lead to the well-known general form of the maximum entropy distribution [38]:

$$p(x) = t(x) \exp\left[\sum_{j=1}^{n} \lambda_j f_j(x) \right]. \tag{4}$$

where the normalization condition on $p(x)$ is enforced by setting $f_1(x) = 1$ and $\mathrm{E}\left[f_1(x) \right] = 1$, and considering a Lagrange multiplier $\lambda_1 = \lambda_1' - 1$. The *n*-Lagrange multipliers are constant values computed by solving a set of *n* simultaneous non-linear equations obtained by substituting Eq. (4) into Eq. (2).

2.2 Family of Maximum Entropy distributions

2.2.2 Basic concepts

The available information might have uncertainty so that the statistical moments are known to lie in a certain domain. For simplicity, let us express the available information by a set of inequality constraints on the statistical expectation:

$$v_{j,\min} \le v_j = \mathrm{E}\left[f_j\left(x\right)\right] = \int f_j\left(x\right) p\left(x\right) \mathrm{d}\, x \le v_{j,\max}, \qquad j = 2,3,...,n \tag{5}$$

where $v_{j,\min}$ and $v_{j,\max}$ are the lower and upper bounds on the jth statistical expectation v_j.

Many distributions can satisfy the inequality constraints specified in Equation (5). The proposed uncertainty description first constructs a family of Maximum Entropy distributions consistent with the statistical inequality constraints, then propagates the family of pdfs through the equations describing the problem on hand in order to yield the pdf which maximizes (or equivalently minimizes) a specified engineering metric.

Specifically, the pdf of a vaguely known variable x is expressed as the exponential of a linear combination of specified functions of the random variable $f_j(x)$ and some bounded variables $\mathbf{a}$ (referred to here as basic variables), so that:

$$p(x|\mathbf{a} \in R) = t(x)\exp\left[\sum_{j=1}^{n} a_j f_j(x)\right]. \tag{6}$$

The basic variables are contained in the vector $\mathbf{a}$, which has entries a_j with $j = 2,3...,n$, and they lie within an admissible region R (which can be an interval, a convex region, etc.). These basic variables substitute the Lagrange multipliers of Eq. (4) and are such that they can have any possible pdf within certain bounds, including the extreme case of a delta function at any point between the bounds. Therefore, Eq. (6) represents a family of Maximum Entropy distributions defined over the set of basic variables $\mathbf{a}$. If a parameter is not "basic", then its pdf can be expressed in terms of the basic parameters, and thus only this type of parameter is considered in what follows. The term $f_1(x) = 1$, and the coefficient a_1 is dependent on the basic variables a_j (with $j = 2,3...,n$), being chosen to satisfy the normalisation condition.

For ease of presentation, the following analysis adopts a uniform prior in equation (6), so that $t(x) = 1$, although this restriction could readily be relaxed if required. Strictly $t(x) = 1$ corresponds to an "improper prior" [40], in the sense that the prior does not satisfy the normalisation condition, but this does not affect the analysis: the posterior distribution is normalised, and this process absorbs any normalising constant that might be added to the prior.

2.2.2 Constructing a family of Maximum Entropy distributions

When the statistical moments are known to lie in a certain domain (for example as in Eq. (5)), the construction of the family of Maximum Entropy distributions consists of the following steps:

1. Express the pdf of a vaguely known variable in the form of Eq. (6).
2. Convert the statistical moments domain (*m*-domain) into a basic variable domain (so-called *a*-domain).
3. Subdivide the *a*-domain into a sufficient number of grid of points.
4. Compute the coefficient a_1 for each point of the grid (by using the normalisation condition) to derive the corresponding pdf.

In the next subsection a procedure for efficiently performing step 2 is presented.

2.2.3 Treatment of bounds

Consider the case in which the information on the pdf of x is given in terms of a bounded statistical moment, say $v_{2,\min} \le \mathrm{E}\left[f_2(x)\right] \le v_{2,\max}$. The aim of the analysis is to evaluate the mapping to the basic variable domain (*a*-domain) as illustrated in Figure 1.

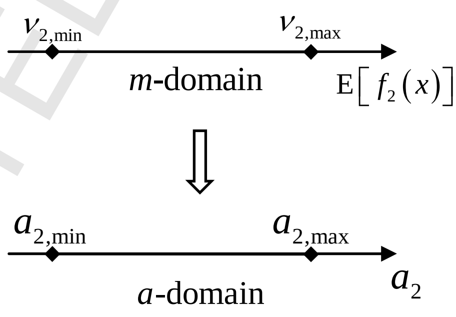

Figure 1: Converting bounds on the statistical expectations $\mathrm{E}\left[f_2(x)\right]$ (*m*-domain) into bounds on the basic variable a_2 (*a*-domain).

According to Eq. (6), for the specified inequality constraint, the pdf is expressed as:

$$p(x|\mathbf{a}) = \exp\left[a_1 + a_2 f_2(x)\right]. \tag{7}$$

ACCEPTED MANUSCRIPT

where a_2 is the unknown basic variable and a_1 is a coefficient which is chosen to satisfy the normalisation condition. By employing the definition of statistical expectation (Eq. (2)), the lower bound on a_2, $a_{2,\min}$, is calculated from the equation

$$\int f_2(x)\exp\left[a_1\left(a_{2,\min}\right)+a_{2,\min} f_2(x)\right]\mathrm{d}\,x = v_{2,\min} \tag{8}$$

Similarly, the upper bound on a_2, $a_{2,\max}$, is obtained from

$$\int f_2(x)\exp\left[a_1\left(a_{2,\max}\right)+a_{2,\max} f_2(x)\right]\mathrm{d}x = v_{2,\max} \tag{9}$$

The mapping into the *a*-domain can become much more computationally demanding when the *m*-domain is expressed as a general region defined by multiple reference points. Consider for example the simple case where the information on the pdf of the uncertain variable x is described via a rectangular *m*-domain, as shown in Figure 2(a).

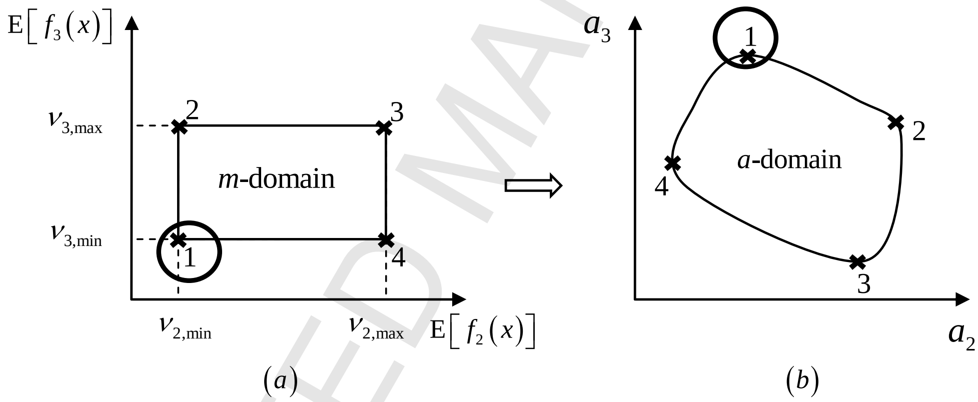

Figure 2: Converting a rectangular *m*-domain (a) into the corresponding *a*-domain (b).

According to Eq. (6), the form of the pdf is now:

$$p(x|\mathbf{a}) = \exp[a_1 + a_2 f_2(x) + a_3 f_3(x)] \tag{10}$$

where a_2 and a_3 are the unknown basic variables, and a_1 is chosen to satisfy the normalisation condition.

Each point of the basic variables domain (*a*-domain), which is depicted in Figure 2(b), can be obtained from the *m*-domain (Figure 2(a)) by solving a set of two non-linear equations in terms of the statistical expectations of the random variable. For example, point 1 of the *m*-domain (Figure 2(a)) can be mapped in the corresponding point 1 of the *a*-domain (Figure 2(b)) by solving:

$$\begin{cases} \int f_2(x)\exp\left[a_1(a_{2,1},a_{3,1})+a_{2,1}f_2(x)+a_{3,1}f_3(x)\right]\mathrm{d}\,x = v_{2,\min} \\ \int f_3(x)\exp\left[a_1(a_{2,1},a_{3,1})+a_{2,1}f_2(x)+a_{3,1}f_3(x)\right]\mathrm{d}\,x = v_{3,\min} \end{cases} \tag{11}$$

A good approximation of the shape of the *a*-domain can be obtained by considering enough sample points along the edges of the *m*-domain. However, even for the simple problem under investigation, the solution of each set of non-linear equations can be time consuming and convergence problems may occur.

A computationally efficient approach is developed here by expressing the variation of the pdf over the *m*-domain as a Taylor series. The mid-point of the *m*-domain is denoted by $\mathbf{v}^*$, and this point will map to a point in the *a*-domain which will be denoted by $\mathbf{a}^*$. The dependency of the pdf on **a** in the vicinity of $\mathbf{a}^*$ is written as a Taylor series in the form:

$$\begin{aligned} p(x|\mathbf{a}) = p(x|\mathbf{a}^*) + \sum_{j=2}^{n}(a_j - a_j^*)\left.\frac{\partial p(x|\mathbf{a})}{\partial a_j}\right|_{\mathbf{a}^*} + \\ +\frac{1}{2}\sum_{j=2}^{n}\sum_{k=2}^{n}(a_j-a_j^*)(a_k-a_k^*)\left.\frac{\partial^2 p(x|\mathbf{a})}{\partial a_j \partial a_k}\right|_{\mathbf{a}^*} \\ +\frac{1}{6}\sum_{j=3}^{n}\sum_{k=3}^{n}\sum_{l=3}^{n}(a_j-a_j^*)(a_k-a_k^*)(a_l-a_l^*)\left.\frac{\partial^3 p(x|\mathbf{a})}{\partial a_j \partial a_k \partial a_l}\right|_{\mathbf{a}^*} + \ldots \end{aligned} \tag{12}$$

where $p(x|\mathbf{a}^*)$ is the distribution evaluated at the mid-point of the *m*-domain. As an example, let's consider the case depicted in Figure 3.

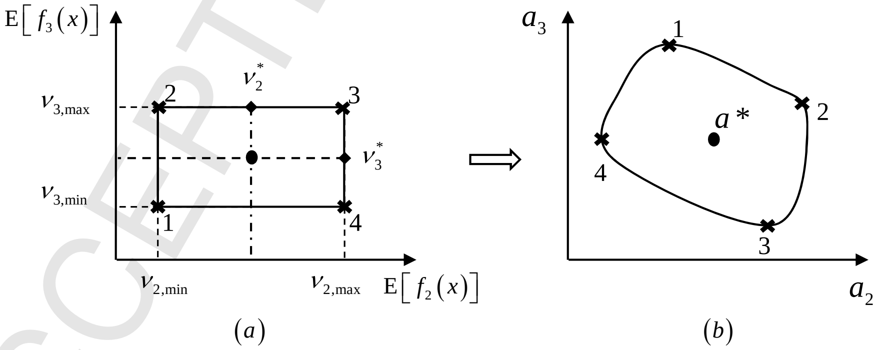

Figure 3: Example of the evaluation of the expansion point. (a) the middle points, v_2^* and v_3^*, of the m-domain are identified. (b) the corresponding point in the *a*-domain is indicated with $\mathbf{a}^*$.

The terms v_2^* and v_3^* specified for the *m*-domain (Figure 3(a)) are employed to yield the term $\mathbf{a}^*$ (depicted in Figure 3(b)), with coordinates a_2^* and a_3^*, by solving a set of two simultaneous equations:

$$\begin{cases} \int f_2(x)\, p\left(x \middle| \mathbf{a}^*\right) \mathrm{d}\, x = v_2^* \\ \int f_3(x)\, p\left(x \middle| \mathbf{a}^*\right) \mathrm{d}\, x = v_3^* \end{cases} \tag{13}$$

The statistical expectation of a function $f_s(x)$ can now be approximated by truncating the Taylor series expansion to the second order term:

$$\begin{aligned} v_s(\mathbf{a}) = \int f_s(x)\, p\left(x \middle| \mathbf{a}\right) \mathrm{d}x = \int f_s(x)\, p\left(x \middle| \mathbf{a}^*\right) \mathrm{d}x + \sum_{j=2}^{n} \left(a_j - a_j^*\right) \int f_s(x) \left.\frac{\partial p\left(x \middle| \mathbf{a}\right)}{\partial a_j}\right|_{\mathbf{a}^*} \mathrm{d}x \\ + \frac{1}{2} \sum_{j=2}^{n} \sum_{k=2}^{n} \left(a_j - a_j^*\right)\left(a_k - a_k^*\right) \int f_s(x) \left.\frac{\partial^2 p\left(x \middle| \mathbf{a}\right)}{\partial a_j \partial a_k}\right|_{\mathbf{a}^*} \mathrm{d}x \\ s = 1, 2, \ldots n \end{aligned} \tag{14}$$

Expressions for the derivatives of the probability density function with respect to the basic variables can be derived by considering the relationship between the basic variables and moments and cumulants of the pdf (as shown in appendix A). Eq. (14) can be finally rewritten as:

$$\begin{aligned} v_s(\mathbf{a}) = c_s^1\left(\mathbf{a}^*\right) - \sum_{j=2}^{n} \left(a_j - a_j^*\right) c_{s,j}^2\left(\mathbf{a}^*\right) - \frac{1}{2} \sum_{j=2}^{n} \sum_{k=2}^{n} \left(a_j - a_j^*\right)\left(a_k - a_k^*\right) c_{s,j,k}^3\left(\mathbf{a}^*\right) \\ s = 1, 2, \ldots n \end{aligned} \tag{15}$$

where $c_s^1\left(\mathbf{a}^*\right), c_{s,j}^2\left(\mathbf{a}^*\right)$ and $c_{s,j,k}^3\left(\mathbf{a}^*\right)$ are the first, second and third order cumulants, respectively, calculated at the $\mathbf{a}^*$ point. The term $c_s^1\left(\mathbf{a}^*\right)$ corresponds to the statistical expectation calculated at $\mathbf{a}^*$, therefore it is equivalent to the term $v_s\left(\mathbf{a}^*\right) = v_s^*$ which can be obtained directly from the *m*-domain, while $c_{s,j}^2\left(\mathbf{a}^*\right)$ and $c_{s,j,k}^3\left(\mathbf{a}^*\right)$ are calculated by the numerical integration of:

$$c_{s,j}^2\left(\mathbf{a}^*\right) = \int \left(f_s(x) - v_s^*\right)\left(f_j(x) - v_j^*\right) p\left(x \middle| \mathbf{a}^*\right) \mathrm{d}\, x, \tag{16}$$

$$c_{s,j,k}^3\left(\mathbf{a}^*\right) = \int \left(f_s(x) - v_s^*\right)\left(f_j(x) - v_j^*\right)\left(f_k(x) - v_k^*\right) p\left(x \middle| \mathbf{a}^*\right) \mathrm{d}\, x. \tag{17}$$

Each point of the *a*-domain $\mathbf{a}$ corresponding to a point $v(\mathbf{a})$ of the *m*-domain can be then computed by solving a set of *n* (where *n* corresponds to the domain dimension) equations (in the form of Eq. (15)) where a linear or quadratic approximation might be considered. High order terms may also be included by using the relations in appendix A. Therefore, if *r* points of a 3-dimensional *m*-domain are mapped into the *a*-domain, this would require solving *r* sets of 3 equations.
By adopting this approach, the edges of the *m*-domain can be mapped to the *a*-domain in an efficient way, thus allowing a permissible region of the *a*-domain to be determined.
The foregoing mapping procedure (which forms step 2 of the overall process listed in subsection 2.2.2) can be summarized as follows:

1. Map the mid-point of the *m*-domain ($\mathbf{v}^*$) to a point in the *a*-domain $\mathbf{a}^*$ by solving a set of non-linear equations in terms of the statistical expectations of the random variable. These equations will each have the form of those shown in Eq. (13).
2. Calculate the cumulants $c^2_{s,j}(\mathbf{a}^*)$ and $c^3_{s,j,k}(\mathbf{a}^*)$ (Eq. (16) and Eq. (17)).
3. Compute the edges of *a*-domain by considering a set of points on each edge of the *m*-domain. At each point a set of *n* (where *n* corresponds to the domain dimension) equations in the form of Eq. (15) is used to map the *m*-coordinates to the *a*-coordinates.

The steps for generating the family of Maximum Entropy distributions (subsection 2.2.2), including the treatment of bounds just described, are illustrated via a numerical example in the following subsection. The family of pdfs generated in the next subsection will then be used in a number of numerical applications in section 3.

2.2.4 Generating the family of Maximum Entropy distributions: example

Let us consider an elastic spring x with the following available information:
(i) the variable is positive
(ii) the vertices of a convex region of the statistical expectations $\mathrm{E}[x]$ and $\mathrm{E}[\ln(x)]$ are known, as specified in Table 1 and shown in Figure 4.

Vertices of the *m*-domain	Coordinates (N/m; -)
1	$(18.0\times10^5, 14.273)$
5	$(22.0\times10^5, 14.518)$
9	$(22.0\times10^5, 14.498)$
13	$(18.0\times10^5, 14.243)$

Table 1: Statistical expectation domain (*m*-domain) vertex coordinates

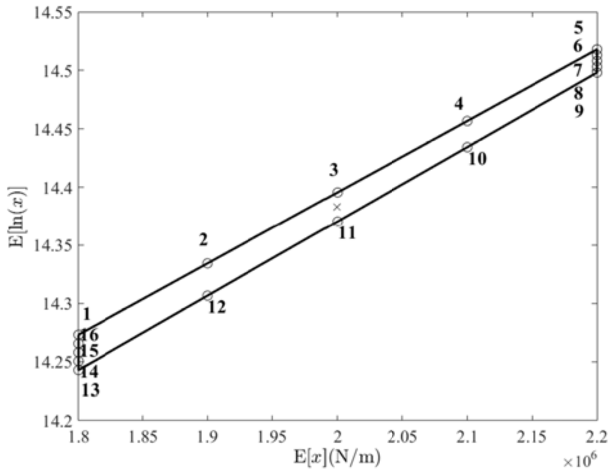

Figure 4: Statistical expectation domain (*m*-domain). The circles indicate points along the *m*-domain, while the "x" indicates the middle point of the *m*-domain

This *m*-domain displays a maximum variation of 10% on $\mathrm{E}[x]$ and of 0.95% on $\mathrm{E}\left[\ln(x)\right]$ with respect to the corresponding mid-points $\mathrm{E}\left[x^*\right]=20.0\times10^5$ N/m and $\mathrm{E}\left[\ln(x)^*\right]=14.383$ .The family of Maximum Entropy pdfs are generated following the procedure described in subsection 2.2.2:

Step 1: Express the pdf of a vaguely known variable in the form of Eq. (6).
The pdf of x is written in the same form of Equation (6), that is a Gamma distribution:

$$p(x|\mathbf{a}) = \exp[a_1 - a_2 x - a_3 \ln(x)], \tag{18}$$

where a_2 and a_3 are the two unknown basic variables, while a_1 is obtained by applying the normalisation condition (for $\mathrm{Re}[a_2] > 0; \mathrm{Re}[a_3] < 1$) as:

$$a_1 = -\ln\left(a_2^{(a_3-1)}\Gamma(1-a_3)\right), \tag{19}$$

where $\Gamma(\bullet)$ is the gamma function.
The moments of the gamma function can be expressed in closed-form in terms of the basic variables:

$$E[x] = \frac{1-a_3}{a_2} \tag{20}$$

$$E[\ln(x)] = \psi(1-a_3) - \ln(a_2) \tag{21}$$

where $\Psi(\bullet)$ is the digamma function. Therefore Eq. (20) and Eq. (21) can be used to compute the *a*-domain exactly. These equations will be used in what follows to verify the approximate mapping strategy proposed.

Step 2: Convert the statistical moments domain (*m*-domain) into a basic variable domain (so-called *a*-domain).

Although the *m*-domain is characterized by linear surfaces, the corresponding *a*-domain is not; therefore, three points for every two vertices (at 1/4, 1/2 and 3/4 from one of the vertices) of the *m*-domain are considered. These points are shown in Figure 4.

The proposed mapping strategy (described in section 2.2.4) would consider a Taylor series expansion over the whole domain, taking the mid-point of the domain as the reference point for the expansion. For the present example the value of $\mathbf{a}^* = \left(a_2^*, a_3^*\right)$ corresponding to the mid-point is found by solving the equations:

$$\begin{cases} \int x \exp\left[a_1^* + a_2^* x + a_3^* \ln(x)\right] \mathrm{d}\,x = \mathrm{E}\left[x^*\right] = 19.999 \times 10^5 \\ \int \ln(x) \exp\left[a_1^* + a_2^* x + a_3^* \ln(x)\right] \mathrm{d}\,x = \mathrm{E}\left[\ln\left(x^*\right)\right] = 14.383 \end{cases} \tag{22}$$

indicated with an “x” in Figure 4. The solution of Eq. (22) leads to $\mathbf{a}^* = \left(20.696 \times 10^5, -3.139\right)$. This has been calculated using the Matlab function “fsolve” [41] which finds the roots of a system of non-linear equations by applying the trust-region dogleg algorithm [41], and it has been verified using Eq. (20) and Eq. (21). Each of the 16 points labelled in the *m*-domain in Figure 4 is then mapped onto the *a*-domain by solving a set of two quadratic equations expressed as in Equation (15). Each point in the *a*-domain has been verified by exploiting the direct relation between statistical moments and basic variables (Eq. (20) and Eq. (21)) showing a good agreement (a perfect agreement can only be reached if the moments are a quadratic function of the basic variables). The *a*-domain so obtained is shown in Figure 5.

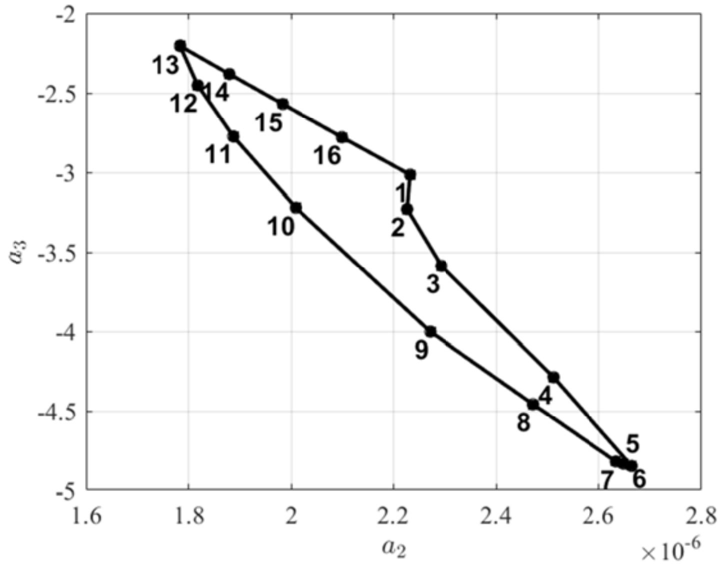

Figure 5: Basic variable domain (a-domain)

Step 3: Subdivide the a-domain into a sufficient number of grid of points.
The a-domain is then enclosed within a rectangle (shown with dashed lines in Figure 6(a)), and a grid of 50×50 equally-spaced points was considered. 414 of these points were inside the a-domain (as shown in Figure 6(a)).

Step 4: Compute the coefficient a_1 for each point of the grid (by using the normalisation condition) to derive the corresponding pdf.
These points and the 16 points along the a-domain, produced a family of 430 pdfs (40 pdfs belonging to this family are shown in Figure 6(b).

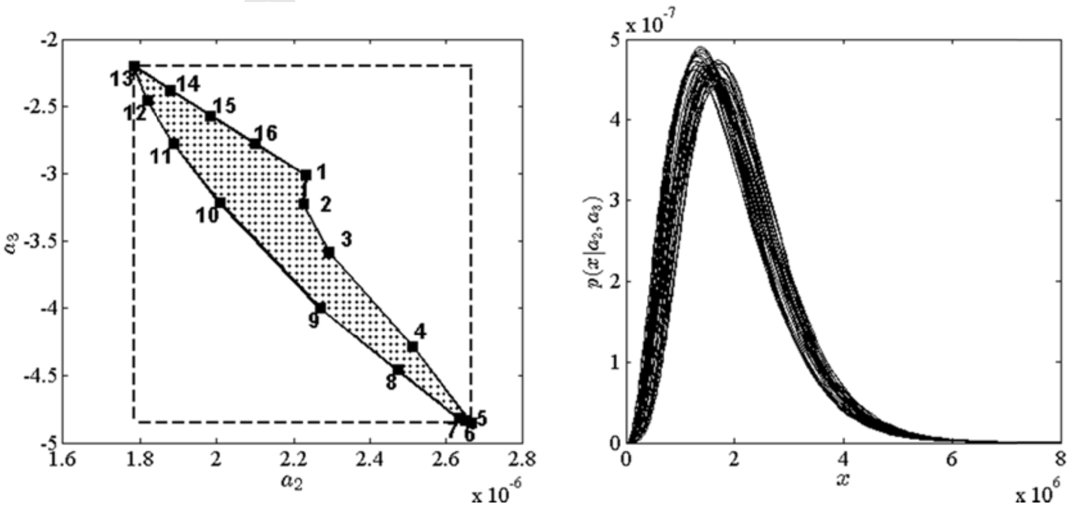

(a) (b)

Figure 6: Points sampled within the *a*-domain (a). 40 pdfs obtained from 40 random points taken within the *a*-domain (b)

The set of 430 pdfs generated is used in the next sections to investigate the performance of engineering systems.

The Maximum Entropy distribution, which is the gamma pdf with the largest entropy that satisfies the statistical moment conditions, can be computed by calculating the entropy (measured in nats) associated with each gamma distribution:

$$h_e = \ln\left(\frac{\Gamma(1-a_3)}{a_2}\right) + a_3\Psi(1-a_3) + 1 - a_3 \tag{23}$$

and then searching in the *a*-domain (or equivalently in the *m*-domain by using Eq. (20) and Eq. (21)), the combination of basic variables which maximise Eq. (23). For the case under investigation, the pdf with the largest entropy is the one with basic variables corresponding to point 10 of the *a*-domain.

3 Performance analysis of engineering systems

The feasibility of the proposed uncertainty model is shown in this section through its application to three engineering problems: (i) fatigue failure analysis of a structural joint; (ii) evaluation of the probability that a response variable of an engineering system exceeds a critical level, and (iii) random vibration.

3.1 Fatigue failure of a structural joint

Fatigue failures of structural joints are caused by excessive accumulated damage produced by fluctuating stresses due to time-varying loadings (for example ocean wave loads acting on an offshore structure). These stresses are usually random and difficult to be fully characterised, given the random nature of the loadings acting on the structures, the uncertainty in the dynamical properties of the structures itself and the inherent variability in the fabrication of structural joints. The average damage caused at a joint of a structure in a time T by a random stress S, $\mathrm{E}[D(T)]$, is proportional to the average of the inverse of the number of stress level at amplitude S, $N(S)$, which are required to produce a failure [42-43]:

$$\mathrm{E}[D(T)] \propto \int_0^\infty \frac{p(S)}{N(S)}\mathrm{d}S \tag{24}$$

where $p(S)$ is the distribution of peak stress amplitude, and $N(S)$ is obtained from the characteristic *S-N* curve of the joint [41,42]. In particular, $N(S)$ is usually expressed in the form [42,43]

$$N(S) = CS^{-m} \tag{25}$$

where C and m are fatigue coefficients which can be derived experimentally or can be obtained from the classified *S-N* curves [42,43]. Equation (24) can be therefore rewritten as

$$\mathrm{E}[D(T)] \propto \int_0^{\infty} S^m p(S)\,\mathrm{d}S \tag{26}$$

Let us now assume that the pdf of the stress level in the joint is imprecisely known and is expressed as $p(S|\mathbf{a}) = p(x|\mathbf{a})$. The average damage can now be expressed as:

$$\mathrm{E}[D(T)|\mathbf{a}] \propto \int_0^{+\infty} S^m p(S|\mathbf{a})\,\mathrm{d}S \tag{27}$$

A fatigue failure function can be then introduced:

$$F(\mathbf{a}) = \int_0^{+\infty} S^m p(S|\mathbf{a})\,\mathrm{d}S - \mathrm{t} > 0 \tag{28}$$

where t is a fixed threshold, specified according to the problem on hand, that if exceeded leads to a fatigue damage “failure”.
The aim of the analysis is then to predict the maximum and minimum values of the fatigue failure function:

$$\min_{\mathbf{a}\in R} F(\mathbf{a}) \le F \le \max_{\mathbf{a}\in R} F(\mathbf{a}) \tag{29}$$

Moreover, if a large number of pdfs is producing fatigue failures, then two options can be explored: (i) gain more information in order to reduce, if possible, the basic variable domain; (ii) investigate the behaviour of a different structural joint.

3.1.1 Numerical application on fatigue failure

Consider a stress level in the joint with a pdf as the one described in subsection 2.2.4. The fatigue coefficient m is set to 3.5 and a threshold of $\mathrm{t} = 2.8 \times 10^{22}$ is specified. By using Equation (28) it is found that 179 pdfs, out of the 430 pdfs generated, lead to a fatigue failure. Each pdf is fully identified by specifying (a_2, a_3), therefore each pdf leading to a fatigue failure can be identified by a point in the *a*-domain. This type of description is used in Figure 7, where each pdf leading to fatigue failure is indicated in with a black marker. The maximum and minimum values of the fatigue failure function (obtained from Equation (29) and specified in Figure 7 with the labels “max” and “min” and grey circles) are, respectively, 3.3134×10^{22} and 2.8015×10^{22}.

If the MaxEnt distribution (corresponding to point 10 of the *a*-domain and indicated with the label "MaxEnt" in Figure 7) is used to represent the distribution of the stress amplitude in Equation (28), it would yield 3.1460×10^{22}. The MaxEnt distribution would therefore underestimate the maximum value of the fatigue function.

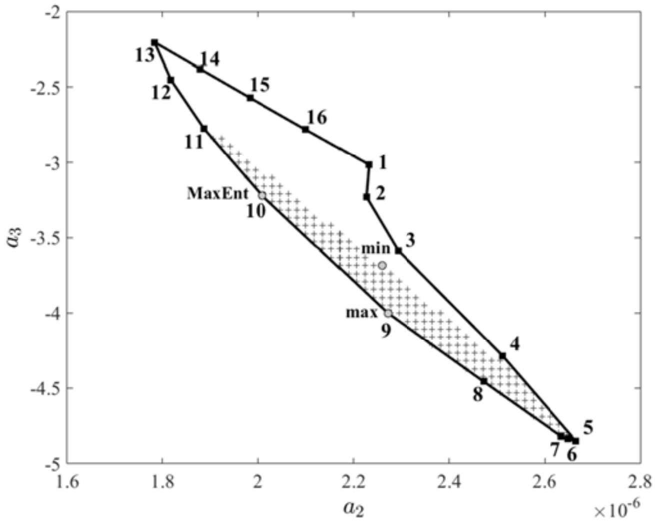

Figure 7: Fatigue failure analysis results. The pdfs which yield to fatigue failure are indicated in the *a*-domain by cross markers. The pdfs that produce to the minimum and maximum failure functions are indicated with min and max, respectively, and a grey circle. The maximum entropy pdf is indicated with MaxEnt

3.2 Failure probability estimation

The performance of an engineering system is generally uncertain due to the uncertainties in the loading, boundary conditions and in the material and geometrical properties of the system. Therefore, the performance is usually expressed in terms of the probability that the design targets will be met [1]. Equivalently, the failure probability, P_f, can be used:

$$P_f = \mathrm{Prob}[\, w \geq w_0 \,] = \int_{w_0}^{\infty} p(\, w\,)\,\mathrm{d}w \tag{30}$$

that is the probability that the response variable w of an engineering system exceeds a critical level w_0, where $p(\, w\,)$ is the distribution of the response variable obtained by propagating the uncertainty in the input variables $p(\, \mathbf{y}\,)$.

If the input pdfs are vaguely known, the uncertainty in the pdf assignment produces uncertainties in the pdf of the response variable. Therefore, the failure probability estimate is itself subject to uncertainty. By employing the proposed imprecise probability description, a family of input pdfs is constructed over the basic variable domain $p(\mathbf{y}|\mathbf{a})$. For fixed basic variables, the pdf of the response variable $p(w|\mathbf{a})$ can be established, and consequently the failure probability conditional on the basic variable is estimated as:

$$P_f(\mathbf{a}) = \mathrm{Prob}[w|\mathbf{a} \geq w_0] = \int_{w_0}^{\infty} p(w|\mathbf{a})\mathrm{d}w \tag{31}$$

Finally, the upper and lower bounds on the failure probability can be evaluated as:

$$\min_{\mathbf{a}\in R}\left(P_f(\mathbf{a})\right) \leq P_f \leq \max_{\mathbf{a}\in R}\left(P_f(\mathbf{a})\right). \tag{32}$$

These bounds provide an indication of the effects of the uncertain input pdf on the failure probability estimate, and allow establishing the highest failure probability to be expected which would be of more interest from an engineering point of view.

3.2.1 Numerical application on failure probability

Let us consider again the spring stiffness described in subsection 2.2.4. It is assumed that the failure condition is reached when the spring stiffness x exceeds the limit level $x_0 = 4\times10^6$ N/m (overstress failure). The pdfs which yield the maximum (dashed line, corresponding to point 9 of the *a*-domain depicted in Figure 5) and minimum (dotted line, corresponding to point 1 of the *a*-domain depicted in Figure 5) failure probabilities are shown in Figure 8, where also the MaxEnt pdf (continuous black line, corresponding to point 10 of the *a*-domain depicted in Figure 5) is shown.

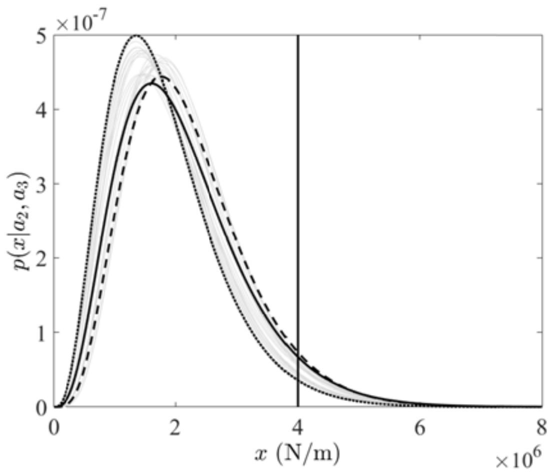

Figure 8: Set of probability density functions (pdfs) compared to a limit level (vertical continuous line). Dashed line: pdf that yield the maximum failure

probability. Dotted line: pdf that yield the minimum failure probability. Continuous black line: maximum entropy pdf

It has been found that $0.0227 \leq P_f \leq 0.0522$ while, the failure probability obtained by considering the MaxEnt pdf is 0.0509. A difference of about 56% can be observed between the upper and lower bounds of the failure probability, meaning that including the imprecise probability descriptions significantly affects the failure probability estimates. Also for this case, the MaxEnt pdf would lead to underestimating the upper bounds of the engineering metric of interest.

3.3 Random vibration analysis

In the design of aircraft structural components is often assumed that only the randomness in the excitation (of mechanical and acoustic nature) is of concern, while the parameters of the structural components are assumed to be deterministic. The random vibration analysis of aircraft structural components is often performed with simplified techniques, such as Miles' Equation [44], which assumes that a structural component, or a secondary structure, has a dominant natural frequency with respect to the structural response.

The random vibration analysis of aircraft structural components reduces to the study of a Single Degree of Freedom (SDOF), consisting of a mass m, a spring k and a damper c, subject to a random external force $F(t)$ which produces a displacement of the mass $y(t)$, as shown in Figure 9.

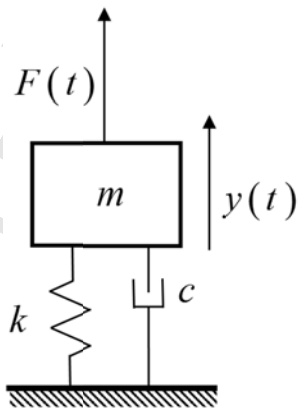

Figure 9: Damped SDoF subject to a force

The governing equation of the problem can be written as:

$$\ddot{y}(t) + 2\zeta\omega_n \dot{y}(t) + \omega_n y(t) = \frac{F(t)}{m} \tag{33}$$

being $\zeta = c/\left(2\sqrt{k\ m}\right)$ the damping ratio, and $\omega_n = \sqrt{k/m} = 2\pi \bar{f}_n$ the SDOF natural frequency corresponding to the dominant natural frequency of the structural component.

If the input is a broadband random loading with a constant spectral density over the frequency range of interest, $S_{FF}\left(\bar{f}\right) = S_0$ (with units of $\left(\mathrm{N}/kg\right)^2/\mathrm{Hz}$), being $\bar{f}$ the frequency expressed in Hz, the solution of the SDoF governing equation yields the Miles' Equation [44]:

$$\sigma_y = y_{rms} = \sqrt{\frac{QS_0\left(\bar{f}_n\right)}{32\pi^3 \bar{f}_n^{\,3}}} \tag{34}$$

This equation expresses the root mean square (rms) of the mass displacement, σ_y as a function of the natural frequency of the SDoF, $\bar{f}_n$, of the quality factor $Q = 1/\left(2\zeta\right) = \left(\sqrt{k\ m}\right)/c$ and of the value of the excitation force spectral density at the natural frequency $S_0\left(\bar{f}_n\right)$.

In aircraft design it is important to verify that the structure is be able to withstand a certain stress levels, such as the yield stress. We can now define the failure probability of the structural component, as the probability that the displacement $y(t)$ exceeds a given level b with a velocity $\dot{y}(t)$ in a certain period of time τ. It is well known that by assuming that each crossing of the barrier is independent from each other and randomly distributed along the time axis, the failure probability P_f can be expressed as [42-44]:

$$P_f = 1 - \exp\left[-\nu_b^+ \tau\right] \tag{35}$$

Being ν_b^+ the average number of positive crossing per unit of time of a barrier *b*, which is given by [42-44]

$$\nu_b^+ = \frac{\sigma_{\dot{y}}}{2\pi\sigma_y} \exp\left[-\frac{1}{2}\left(\frac{b}{\sigma_y}\right)^2\right] \tag{36}$$

Here $\sigma_{\dot{y}}$ is the mean square of the velocity which is given by [41-43]:

$$\sigma_{\dot{y}} = \sqrt{\frac{S_0}{8\zeta\left(2\pi \bar{f}_n\right)}} \tag{37}$$

Nonetheless, the dominant frequency of the system may be uncertain because of manufacturing variability, and because of variation in joints and connections of structural components. This conventional approach is extended here in two ways: (i) firstly, the system parameters are taken to be uncertain rather than known, (ii) secondly, the uncertainty is modelled with an imprecise probability description, rather than with conventional pdfs (which usually are not known, due to a lack of empirical information).

When the system parameters are modelled with a probability density function, the problem concern with an ensemble of SDoFs. Each element of the ensemble has a specified value of the natural frequency, and when subject to the random loading, it is characterised by a random displacement response.

If we assume $\overline{f}_n$ is described by a probability distribution $p\left(\overline{f}_n\right)$, we can then apply two different methods:

Method A – unconditional failure probability

Method A enables the evaluation of the unconditional failure probability across an ensemble of SDoFs. This achieved by solving the unbounded integral:

$$\overline{P}_f = \int P_f\left(\overline{f}_n\right) p\left(\overline{f}_n\right) \mathrm{d}\overline{f}_n \tag{38}$$

where $P_f\left(\overline{f}_n\right)$ is the failure probability of a member of the ensemble (for fixed $\overline{f}_n$) which is computed using Eq. (35). This type of integral can be evaluated numerically by considering a grid of integration points (direct integration) or by employing Monte Carlo Simulations [1].

Method B – probability of failure probability exceeding a target level

Method B yields the probability that the failure probability exceeds a specified target level θ across the ensemble of SDoFs. This is expressed as a bounded integral:

$$P\left[P_f > \theta\right] = \int_{P_f > \theta} p\left(\overline{f}_n\right) \mathrm{d}\overline{f}_n \tag{39}$$

In most cases the analytical solution of this integral is not known and its approximate solution can be obtained by using numerical integration methods or Monte Carlo Simulations [1].

Method A addresses the problem of estimating the probability that a deterministic limit value of the SDoF displacement response is exceeded by the response variable across the ensemble of SDoFs; Method B addresses a different type of problem: by specifying a critical value of the failure probability, it yields the probability that the failure probability itself exceeds this critical value. Therefore, these approaches yield two probability estimates which can be very useful from the engineering point of view.

By introducing uncertainty in the probabilistic assignment of the system parameters, using the form $p\left(\bar{f}_m \middle| \mathbf{a}\right)$, Method A and Method B can be generalised to yield bounded quantities.

Generalisation of Method A

For fixed basic variables $P_f\left(\bar{f}_n \middle| \mathbf{a}\right)$ can be established, then Equation (38) can be generalised to yield the unconditional failure probability for fixed basic variables:

$$\bar{P}_f(\mathbf{a}) = \int P_f\left(\bar{f}_n \middle| \mathbf{a}\right) p\left(\bar{f}_n \middle| \mathbf{a}\right) \mathrm{d}\bar{f}_n \tag{40}$$

As a result we can then evaluate the upper and lower bounds on the failure probability as:

$$\min_{\mathbf{a}\in R}\left(\bar{P}_f(\mathbf{a})\right) \le \bar{P}_f \le \max_{\mathbf{a}\in R}\left(\bar{P}_f(\mathbf{a})\right) \tag{41}$$

These bounds provide an indication of the effects of the uncertainty in the natural frequency pdf to the system reliability. As a result, the designer can decided to (i) gain more information on the vaguely known pdf in order to reduce, if possible, the basic variable domain; (ii) investigate a different design solution to reduce the maximum failure probability, if this is not acceptable.

Generalisation of Method B

Equation (39) can be also generalised to yield the probability that the failure probability exceed a certain threshold θ for fixed basic variables $\mathbf{a}$:

$$P\left[\left(P_f > \theta\right) \middle| \mathbf{a}\right] = \int_{P_f > \theta} p\left(\bar{f}_n \middle| \mathbf{a}\right) \mathrm{d}\bar{f}_n \tag{42}$$

to yield the following bounds:

$$\min_{\mathbf{a}\in R}\left(P\left[\left(P_f > \theta\right)\middle|\mathbf{a}\right]\right) \le P\left[\left(P_f > \theta\right)\right] \le \max_{\mathbf{a}\in R}\left(P\left[\left(P_f > \theta\right)\middle|\mathbf{a}\right]\right) \tag{43}$$

These bounds provide an indication on the confidence on having reached a reliability target level (probability of exceedance of a limit failure probability value) given the uncertainty in the pdf. The narrow they are, the more confident the designer can be about the reliability target level.

3.3.1 Numerical application

Consider a structural panel of a spacecraft with fundamental frequency of $\overline{f}_n$ =250 Hz, damping ratio $\zeta = 0.05$ (quality factor $Q = 10$), subject to a white noise Power Spectral Density function $S_0 = 100\ (\mathrm{N}/kg)^2 / \mathrm{Hz}$. A displacement threshold level $b = 7 \times \sigma_y = 0.0018$ mm (σ_y being computed with Eq. (34)) during a time interval $\tau = 3$ hours is specified.
Using the standard approach (Eq. (35)), the resulting failure probability is: $P_f = 6.1 \times 10^{-5}$.
Now, let us consider that the fundamental frequency of the panel is imprecisely known, and it is defined in terms of the spring stiffness described in subsection 2.4, so that the pdf of the natural frequency conditional on the basic variables, $p(\overline{f}_n | \mathbf{a})$, is given by (see appendix B for its derivation):

$$p(\overline{f}_n | \mathbf{a}) = 2\gamma \overline{f}_n \exp\left[a_1 - a_2 \gamma \overline{f}_n^{\,2} - a_3 \ln\left(\gamma \overline{f}_n^{\,2} \right) \right], \tag{44}$$

where $\gamma = 4\pi^2 m$ with $m = 0.81$ kg, and a_1 is obtained by applying the normalisation condition (for $\mathrm{Re}[a_2] > 0; \mathrm{Re}[a_3] < 0$) as:

$$a_1 = \ln\left(\frac{a_2 \gamma^{a_3} (a_2 \gamma)^{-a_3}}{\Gamma(1 - a_3)} \right). \tag{45}$$

If we consider a single distribution at point 5, shown as a continuous black line in Figure 10, this would yield a failure probability of: $\overline{P}_f |_{\text{point 5}} = 0.2159$ (obtained solving Eq. (38) using direct integration). Alternatively, by choosing the maximum entropy distribution (shown with a dashed line in Figure 10), this would yield a failure probability of: $\overline{P}_f |_{\text{point 10}} = 0.2935$.

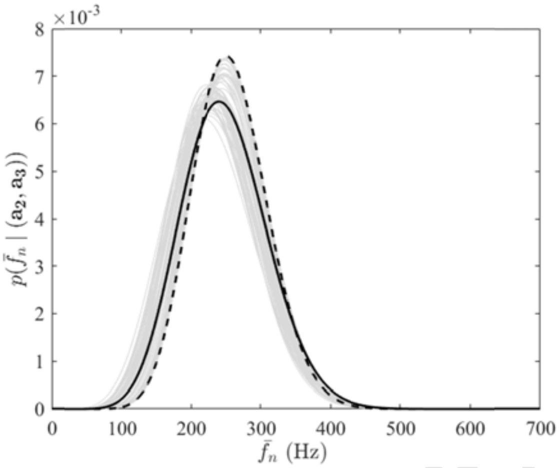

Figure 10: Set of probability density functions (pdfs) of the natural frequency. Dashed line: pdf at point 5 of the *a*-domain. Continuous black line: maximum entropy pdf (point 10 of the *a*-domain)

These results can be explained by considering the sharp variation of the P_f (Eq. (35)) close to 250 Hz (initial deterministic value), as shown in Figure 11.

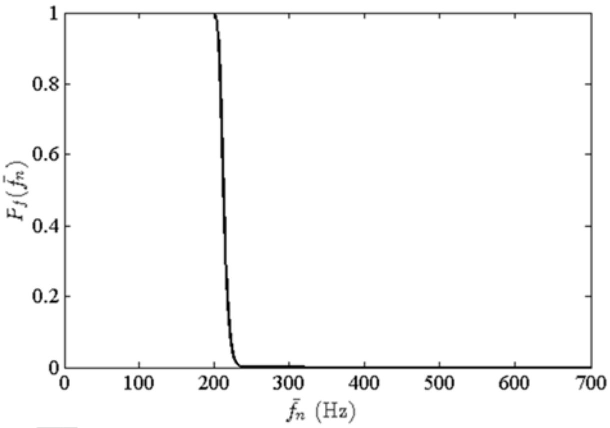

Figure 11: P_f as a function of frequency

If we now set a failure probability target $\theta = 0.001$, the probability of exceedance of this target (obtained solving Eq. (39) using numerical integration) at point 5 and point 10 is: $P\left[\left(P_f > \theta\right)\right]\Big|_{\text{point 5}} = 0.3928$ and $P\left[\left(P_f > \theta\right)\right]\Big|_{\text{point 10}} = 0.4605$.

By letting varying the basic variable within the *a*-domain (using the 430 distribution constructed in subsection 2.2.4), it has been found that the unconditional failure probability can take values between $0.2126 \le \bar{P}_f \le 0.4303$ (obtained at points 7 and

13, respectively); therefore the MaxEnt pdf ($\bar{P}_f\big|_{\text{point 10}} = 0.2935$) would underestimate the upper bound.
Similarly, by using the 430 distribution constructed in section 2.2.4, the probability that the failure probability target is exceeded can vary from $0.3876 \le P\left[\left(P_f > \theta = 0.001\right)\right] \le 0.5918$ (obtained at points 7 and 13, respectively); also in this case the MaxEnt pdf would underestimate the response upper bound ($P\left[\left(P_f > \theta\right)\right]\Big|_{\text{point 10}} = 0.4605$).

It can be concluded that employing the proposed uncertainty model enable an enhanced description of structural panel performance yielding the maximum and minimum values that the engineering metric of interest (eg the failure probability) might take based on the available information, rather than yielding a single value which might significantly underestimate or overestimate the engineering metric of interest.

4 Conclusions

A generalization of Maximum Entropy distribution under uncertain statistical information has been presented in this paper. When the available information has uncertainty such that the statistical moments are known only to lie in a certain domain, Maximum Entropy would yield a single distribution (the MaxEnt pdf) with the largest entropy. As a results, MaxEnt would use the information at only a single point in the domain and would discard the other information. The proposed approach instead uses this information to construct a family of Maximum Entropy distributions, leading to an uncertain probability density function. Therefore, instead of investigating the effects of the MaxEnt pdf on the response variable, the proposed approach yields the pdf which maximizes (or equivalently minimizes) an engineering metric, and quantifies the effect of the uncertain pdf on the response.

A strategy for efficiently treating bounds on the statistical moments to yield the bounds on the parameters of the uncertain pdf has been presented and applied to a vaguely known spring stiffness distribution. The proposed uncertainty model was then applied to: (i) fatigue failure analysis of a structural joint; (ii) evaluation of the probability that a response variable of an engineering system exceeds a critical level, and (iii) random vibration analysis of a panel.

It has been also shown that:

(i) the single value response obtained by using the MaxEnt pdf, often used to deal with uncertain variables, can be significantly lower than the upper response bounds obtained with the set of pdfs;
(ii) the upper and lower bounds on the engineering metric can be largely different. As a result of this analysis, the designer can decided to (a) gain more information on the vaguely known pdf in order to reduce, if possible, the basic variable domain; and/or (b) investigate a different design solution

which can be more robust with respect to the design constraints under uncertainties in the models parameters.

(iii) The uncertainty model proposed can be applied to a broad range of mechanics problems, including static and random vibration analysis.

Acknowledgements

This research did not receive any specific grant from funding agencies in the public, commercial, or not-for-profit sectors.

References

[1] R.E. Melchers, Structural reliability analysis and prediction, second edition, Wiley, England, 1999.

[2] R.S. Langley, Unified approach to probabilistic and possibilistic analysis of uncertain systems, Journal of Engineering Mechanics, 126 (2000) 1163 – 1172.

[3] C. Soize, Random matrix theory for modeling uncertainties in computational mechanics, Computer Methods in Applied Mechanics and Engineering, 194 (2005) 3301-3315.

[4] R.S. Langley, V. Cotoni, Response variance prediction in the statistical energy analysis of built-up systems, Journal of the Acoustical Society of America, 115 (2004) 706 – 718.

[5] R.S. Langley, V. Cotoni, Response variance prediction for uncertain vibro-acoustic system using a hybrid deterministic-statistical method, Journal of the Acoustical Society of America, 122 (2007) 3445 – 3463.

[6] A. Cicirello, R.S. Langley, The vibro-acoustic analysis of built-up systems using a hybrid method with parametric and non-parametric uncertainties, Journal of Sound and Vibration, 332 (2013) 2165 – 2178.

[7] A. Cicirello, R.S. Langley, Efficient parametric uncertainty analysis within the hybrid Finite Element/Statistical Energy Analysis method, Journal of Sound and Vibration, 333 (2014) 1698 – 1717.

[8] A. Cicirello, R.S. Langley, Vibro-Acoustic Response of Engineering Structures With Mixed Type of Probabilistic and Nonprobabilistic Uncertainty Models. ASME. ASME J. Risk Uncertainty Part B. 1(4) (2015) 041001-1 - 041001-13.

[9] Soize, Stochastic modeling of uncertainties in computational structural dynamics—Recent theoretical advances, Journal of Sound and Vibration, 332 (2013) 2379 – 2395.

[10] S.S. Rao, L. Berke, Analysis of uncertain structural system using interval analysis, Journal of American Institute of Aeronautics and Astronautics 35 (1997) 727 – 735.

[11] I. Elishakoff, Essay on uncertainties in elastic and viscoelastic structures: From A. M. Freudenthal's criticisms to modern convex modelling, Computers & Structures 56 (1995) 871 – 895.
[12] D. Moens, D. Vandepitte, A fuzzy finite element procedure for the calculation of uncertain frequency-response functions of damped structures: Part 1—Procedure, Journal of Sound and Vibration 288 (2005) 431 – 462.
[13] G. Boole, An investigation of the laws of thought on which are founded the mathematical theories of logic and probabilities, Walton and Maberly, London, 1854.
[14] J.M. Keynes, A Treatise on Probability, Macmillan And Co, London, 1921.
[15] P. Walley, Statistical reasoning with imprecise probabilities, Chapman and Hall, London, 1991.
[16] K. Weichselberger, The theory of interval-probability as a unifying concept for uncertainty, International Journal of Approximate Reasoning, 24(23) (2000) 149-170.
[17] S. Ferson, J. C. Hajagos, Arithmetic with uncertain numbers: rigorous and (often) best possible answer, Reliability Engineering and System Safety, 85 (2004) 135 – 152.
[18] K. Sentz, S. Ferson, Probabilistic bounding analysis in the quantification of margins and uncertainties, Reliability Engineering and System Safety, 96 (2011) 1126 – 1136.
[19] D. Dubois, H. Prade, Possibility Theory: an approach to computerised Processing of Uncertainty, Plenum Press, New York, 1988.
[20] C. Baudrit, D. Dubois, Practical representation of incomplete probabilistic knowledge, Computational Statistics & Data Analysis, 51 (2006) 86-108.
[21] A.P. Dempster, Upper and lower probabilities induced by a multivalued mapping, The Annals of Mathematical Statistics, 38(2) (1967) 325-339.
[22] G. Shafer, A Mathematical Theory of Evidence, Princeton University Press, NJ, 1976.
[23] C. Baudrit, D. Dubois, D. Guyonnet, Joint Propagation and Exploration of Probabilistic and Possibilistic Information in Risk Assessment, IEEE Transaction of Fuzzy Systems, 14 (2006) 593-608.
[24] S. Desterke, D. Dubois, E. Chojnaki. Unifying practical uncertainty representations – Part I: Generalised p-boxes. International Journal of Approximate Reasoning, 49(3) (2008) 649-663.
[25] D. Dubois, H. Prade. When upper probabilities are possibility measures". Fuzzy Sets and Systems, 49 (1992) 65-74.
[26] L.V. Utkin, An uncertainty model of structural reliability with imprecise parameters of probability distributions, Issue ZAMM - Journal of Applied Mathematics and Mechanics / Zeitschrift für Angewandte Mathematik und Mechanik, 84 (2004) 688 – 699.
[27] I.O. Kozine, L.V. Utkin, An approach to combining unreliable pieces of evidence and their propagation in a system response analysis, Reliability Engineering and System Safety, 85 (2004) 103 – 112.

[28] M. Bruns, C.J.J. Paredis, S. Ferson, Computational methods for decision making based on imprecise information, Reliable Engineering Computing Workshop (REC 2006), 2006.
[29] B. Moller, Fuzzy randomness a contribution to imprecise probability, ZAMM - Journal of Applied Mathematics and Mechanics / Zeitschrift fr Angewandte Mathematik und Mechanik, 84(10-11) (2004) 754-764.
[30] M. Beer, M. Zhang, S.T. Quek, S. Ferson, Structural reliability assessment with fuzzy probabilities, In Proceeding of ISIPTA'11 – Seventh International Symposium on Imprecise Probability: Theory and Applications, 2011.
[31] M. Beer, S. Ferson, V. Kreinovich, Imprecise probabilities in engineering analyses, Mechanical Systems and Signal Processing 37 (2013) 4–29.
[32] C. Baudrit, D. Dubois, N. Perrot, Representing parametric probabilistic models tainted with imprecision, Fuzzy Sets and Systems, 159 (2008) 1913-1928.
[33] N. Pedroni, E. Zio, E. Ferrario, A. Pasanisi, M. Couplet. Hierarchical propagation of probabilistic and non-probabilistic uncertainty in the parameters of a risk model. Computers & Structures, 126:199-213, 2013.
[34] C. Jiang, W. X. Li, X. Han, L. X. Liu, P. H. Le, Structural reliability analysis based on random distributions with interval parameters, Computers and Structures, 89 (2011) 2292 – 2302.
[35] Z. Qiu, D. Yang,I. Elishakoff. Probabilistic interval reliability of structural systems. International Journal of Solids and Structures, 45 (2008) 2850 – 2860.
[36] L. V. Utkin, I. Kozine, On new cautious structural reliability models in the framework of imprecise probabilities, Structural Safety, 32 (2010) 411 – 416.
[37] H. Zhang, Interval importance sampling method for finite element-based structural reliability assessment under parameter uncertainties, Structural Safety, 38 (2012) 1 – 10.
[38] E.T. Jaynes, Probability theory – The logic of Science, Cambridge University Press, Cambridge, 2003.
[39] R.S. Langley, Probability Functionals for Self-Consistent and Invariant Inference: Entropy and Fisher Information, IEEE Transaction on Information Theory, 59(7) (2013) 4397-4407.
[40] D.J. Mackay, Information theory, inference and learning algorithms, Cambridge University Press, 2003.
[41] MATLAB. version 7.13.0.564 (R2011b). The MathWorks Inc., Natick, Massachusetts, 2011
[42] Y.K. Lin, Probabilistic theory of structural dynamics, MacGraw-Hill, 1967.
[43] D. Newland, An introduction to random vibrations, spectral and wavelet analysis, Dover Publications, 2005.
[44] J. Wijker, Random Vibrations in Spacecraft Structures Design, Springer, 2009.

Appendix A

This section describes the relationships between the derivatives of a_1 (which is a coefficient dependent on the basic variables a_j, with $j = 2,...,n$) and: (i) the expected values of the functions of the random variables; (ii) the cumulants of the functions of the random variables.

The joint probability density function of a vector of random variables $\mathbf{x}$ can be written as

$$p(\mathbf{x}|\mathbf{a} \in \mathrm{S}) = \exp\left[a_1 + \sum_{j=2}^{n} a_j f_j(\mathbf{x}) \right]. \tag{A.1}$$

The relationships between the statistical expectations of $f_j(\mathbf{x})$ and the derivatives of a_1 are obtained starting from the normalisation condition

$$\int_{-\infty}^{+\infty} ... \int_{-\infty}^{+\infty} p(\mathbf{x}|\mathbf{a}) \mathrm{d}\mathbf{x} = 1 \tag{A.2}$$

The derivative of Eq. (A2) with respect to a_j gives

$$\int_{-\infty}^{+\infty} ... \int_{-\infty}^{+\infty} \left(\frac{\partial a_1}{\partial a_j} + f_j(\mathbf{x}) \right) p(\mathbf{x}|\mathbf{a}) \mathrm{d}\mathbf{x} = 0 \tag{A.3}$$

which yields

$$\frac{\partial a_1}{\partial a_j} = -\int_{-\infty}^{+\infty} ... \int_{-\infty}^{+\infty} f_j(\mathbf{x}) p(\mathbf{x}|\mathbf{a}) \mathrm{d}\mathbf{x} = -\mathrm{E}\left[f_j(\mathbf{x}) \middle| \mathbf{a} \right] \tag{A.4}$$

where $\mathrm{E}\left[f_j(\mathbf{x}) \middle| \mathbf{a} \right]$ is the expected value of $f_j(\mathbf{x})$ conditional on $\mathbf{a}$.

The second derivative of Eq. (A.2) with respect to a_j and a_k gives

$$\int_{-\infty}^{+\infty}...\int_{-\infty}^{+\infty}\left\{\frac{\partial^2 a_1}{\partial a_j \partial a_k}+\left(\frac{\partial a_1}{\partial a_j}+f_j(\mathbf{x})\right)\left(\frac{\partial a_1}{\partial a_k}+f_k(\mathbf{x})\right)\right\}p(\mathbf{x}|\mathbf{a})\,\mathrm{d}\mathbf{x}=0 \qquad \text{(A.5)}$$

Substituting Eq. (A.4) into Eq. (A.5), the second derivative of a_1 is found as

$$\frac{\partial^2 a_1}{\partial a_j \partial a_k}=-\int_{-\infty}^{+\infty}...\int_{-\infty}^{+\infty}\left(f_j(\mathbf{x})-\mathrm{E}\left[f_j(\mathbf{x})|\mathbf{a}\right]\right)\left(f_k(\mathbf{x})-\mathrm{E}\left[f_k(\mathbf{x})|\mathbf{a}\right]\right)p(\mathbf{x}|\mathbf{a})\,\mathrm{d}\mathbf{x} \qquad \text{(A.6)}$$

which can be rewritten in the form

$$\frac{\partial^2 a_1}{\partial a_j \partial a_k}=-\mathrm{E}\left[\left(f_j(\mathbf{x})-\mathrm{E}\left[f_j(\mathbf{x})|\mathbf{a}\right]\right)\left(f_k(\mathbf{x})-\mathrm{E}\left[f_k(\mathbf{x})|\mathbf{a}\right]\right)\right] \qquad \text{(A.7)}$$

Eq. (A.4) and Eq. (A.7) provide a connection between the derivatives of a_1 and the expected values of the functions of the random variables $\mathbf{x}$, $f_k(\mathbf{x})$. In order to avoid complicating the expressions, the expected value of $f_k(\mathbf{x})$ conditional on $\mathbf{a}$, $\mathrm{E}\left[f_k(\mathbf{x})|\mathbf{a}\right]$, will be indicated with $\mathrm{E}\left[f_k(\mathbf{x})\right]$ in what follows.

The derivatives of a_1 are also linked to the cumulants of $\mathbf{f}(\mathbf{x})$. This relationship can be obtained by considering an analogy with the well-known relationship between the cumulants of random variables $\mathbf{y}$, $k_n\left[y_1 y_2 ... y_n\right]$, and the log-characteristic function [42], which is reviewed in what follows.

The characteristic function of several jointly distributed random variables $\mathbf{y}$ with pdf $p(\mathbf{y})$ is a complex function of the real set of parameters $\boldsymbol{\theta}$ and is given by the Fourier transform of the pdf [42]

$$M(\theta_1,\theta_2,...,\theta_n) = \mathrm{E}[\exp(i(\theta_1 y_1 + \theta_2 y_2 + ... + \theta_n y_n))] = \int_{-\infty}^{+\infty} ... \int_{-\infty}^{+\infty} \exp(i(\theta_1 y_1 + \theta_2 y_2 + ... + \theta_n y_n))\, p(y_1 y_2 ... y_n)\, \mathrm{d}\mathbf{y} \tag{A.8}$$

The derivatives of the characteristic function are related to the joint moments of $\mathbf{y}$ via [42]

$$\left(\frac{\partial^n M(\theta_1,\theta_2,...,\theta_n)}{\partial\theta_1 \partial\theta_2 ... \partial\theta_n} \right)_{\theta_1=\theta_2=...=\theta_n=0} = i^n \mathrm{E}[y_1 y_2 ... y_n] \tag{A.9}$$

Taking the log of the characteristic function and expanding it by using a Taylor series lead to the definition of the joint cumulants as the coefficients in the expression:

$$\ln[M(\theta_1,\theta_2,...,\theta_n)] = i\theta_j k_1[y_j] + \frac{1}{2}(i\theta_j)(i\theta_k) k_2[y_j y_k] + ... \tag{A.10}$$

so that

$$\left(\frac{\partial^n \ln[M(\theta_1,\theta_2,...,\theta_n)]}{\partial\theta_1 \partial\theta_2 ... \partial\theta_n} \right)_{\theta_1=\theta_2=...=\theta_n=0} = i^n k_n[y_1 y_2 ... y_n] \tag{A.11}$$

Now Eq. (A.2) can be rewritten in a form similar to Eq. (A.8)

$$Q(\mathbf{a}) = \exp(-a_1) = \int_{-\infty}^{+\infty} ... \int_{-\infty}^{+\infty} \exp\left[\sum_{j=2}^{n} a_j f_j(\mathbf{x}) \right] \mathrm{d}\mathbf{x} \tag{A.12}$$

The derivatives of $Q(\mathbf{a})$ with respect to the basic variables are given by

$$\frac{\partial^n Q(\mathbf{a})}{\partial a_2 \partial a_3 \ldots \partial a_n} = \int_{-\infty}^{+\infty} \ldots \int_{-\infty}^{+\infty} \left(f_2(\mathbf{x}) f_3(\mathbf{x}) \ldots f_n(\mathbf{x}) \right) \exp\left[\sum_{j=2}^{n} a_j f_j(\mathbf{x}) \right] \mathrm{d}\mathbf{x} \qquad \text{(A.13)}$$

which can be rewritten as

$$\frac{\partial^n Q(\mathbf{a})}{\partial a_{j_1} \partial a_{j_2} \ldots \partial a_{j_n}} = \exp(-a_1) \mathrm{E}\left[\left(f_{j_1}(\mathbf{x}) f_{j_2}(\mathbf{x}) \ldots f_{j_n}(\mathbf{x}) \right) \right] \qquad \text{(A.14)}$$

Considering Eq. (A.9) and Eq. (A.14), $Q(\mathbf{a})$ can be considered to be analogous to $M(\boldsymbol{\theta})$. Therefore, by analogy to Eq. (A.10), we can consider a log-characteristic function associated with $Q(\mathbf{a})$, $\ln(Q(\mathbf{a})) = -a_1$, and expand it by using the Taylor series, so that

$$\ln(Q(\mathbf{a})) = -a_1 = -\sum_{j=2}^{n} \frac{\partial a_1}{\partial a_j} a_j - \frac{1}{2} \sum_{j=2}^{n} \sum_{k=2}^{n} \frac{\partial^2 a_1}{\partial a_j \partial a_k} a_j a_k + \ldots \qquad \text{(A.15)}$$

Comparing Eq. (A.15) to Eq. (A.10) the cumulants of the nth order of the functions of the random variables, $c^n_{j_1, j_2, j_3, \ldots, j_n}$, are given by

$$c^n_{j_1, j_2, j_3, \ldots, j_n} = k_n\left[f_{j_1}(\mathbf{x}) f_{j_2}(\mathbf{x}) \ldots f_{j_n}(\mathbf{x}) \right] = -\frac{\partial^n a_1}{\partial a_{j_1} \partial a_{j_2} \ldots \partial a_{j_n}} \qquad \text{(A.16)}$$

The relationships obtained (Eq. (A.4) and Eq. (A.7)), which are special cases of Eq. (A.16), have been used to convert the bounds on the statistical expectations of a function of a random variable into bounds on the basic variables (subsection 2.2.3).

Appendix B

This section describes the evaluation of the probability density function of the natural frequency of a SDoF starting from a stiffness pdf described as Eq. (18).

Given a random variable z with known pdf $p(z)$ and a transformation $y = g(z)$, the pdf of y is obtained from:

$$p(y) = \sum_{z_i} \left. \frac{p(z)}{\left|\frac{\mathrm{dy}}{\mathrm{dz}}\right|} \right|_{z_i = g^{-1}(y)} \tag{B.1}$$

being z_i the roots of the equation $y = g(z)$.

The natural frequency (in Hz) is given by:

$$\overline{f}_n = \frac{1}{2\pi}\sqrt{\frac{k}{m}} \tag{B.2}$$

If $z = k$, $y = \overline{f}_n$ are the two random variables, and $\eta = \frac{1}{2\pi}\sqrt{\frac{1}{m}}$ is a constant factor, then Eq. (B.2) can be rewritten as:

$$y = \eta\sqrt{z} \tag{B.3}$$

By applying Eq (B.1), the pdf of y is obtained as:

$$p(y) = \left. \frac{p(z)}{\frac{\eta}{2\sqrt{z}}} \right|_{z = \left(\frac{y}{\eta}\right)^2} \tag{B.4}$$

Now, by substituting Eq. (B.3) in Eq. (B.4), $p(y|\mathbf{a})$ is obtained as:

$$p(y|\mathbf{a}) = \frac{2y}{\eta^2}\exp\left[a_1 - a_2\left(\frac{y}{\eta}\right)^2 - a_3\ln\left(\left(\frac{y}{\eta}\right)^2\right)\right], \tag{B.5}$$

Finally, indicating $\gamma = 4\pi^2 m$, the $p(\overline{f}_n|\mathbf{a})$ can be expressed as:

$$p(\overline{f}_n|\mathbf{a}) = 2\gamma\overline{f}_n\exp\left[a_1 - a_2\gamma\overline{f}_n^{\,2} - a_3\ln\left(\gamma\overline{f}_n^{\,2}\right)\right], \tag{B.6}$$

where a_2 and a_3 are the two basic variables whose value can be obtained from the *m*-domain, while a_1 is obtained by applying the normalisation condition (for $\mathrm{Re}[a_2] > 0; \mathrm{Re}[a_3] < 0$) as:

$$a_1 = \ln\left(\frac{a_2\gamma^{a_3}(a_2\gamma)^{-a_3}}{\Gamma(1-a_3)}\right), \tag{B.7}$$